24th COBEM - 2017

24th ABCM International Congress of Mechanical Engineering
December 3-8, 2017, Curitiba, PR, Brazil

COBEM-2017-0009
THE PROBLEM IN THE SIMPLIFIED CONSIDERATION OF DISCS IN THE ROTOR DYNAMICS OF LARGE MACHINES

Lucas Gomes Fonçatti
Danielle Raphaela Voltolini
WEG Equipamentos Elétricos S.A. – Energy Division, Department of Development and Technological Innovation – Avenida Prefeito Waldemar Grubba, 3300, Vila Lalau – Jaraguá do Sul-SC, Brazil, 89256-900.
lfoncatti@weg.net
danieller@weg.net

Abstract. *The models used to consider the elements that make up the rotor, especially in the case of discs, significantly affect the calculation of the rotor dynamic behavior of large machines. Components such as fans and flywheels, to quote, are commonly represented by means of rigid symmetric discs, however, this simplification is not always proper. A good example for this case is a radial flow fan whose design commonly has a hub (responsible for the interface with the shaft) and blades that are supported by radial rings. This typical geometry allows an asymmetric mass distribution with respect to the plane of the disc that supports the assembly, and this, along with the low stiffness of the component, may cause the influence of the disc in the gyroscopic effect greater than the expected on the dynamic behavior of the rotor. This paper investigates this behavior through numerical studies carried out using the finite element method, evaluating numerically the influence of this behavior to industrial rotor designs and showing that the consideration of asymmetric discs should be performed in those cases. Without that consideration, there is a risk to execute a project that will exhibit unanticipated behavior during its operation, such as the excitation of an unpredicted critical rotation.*

Keywords: *Rotor dynamics, Large machinery, Electric motor, Gyroscopic effect, Finite elements method*

1. INTRODUCTION

During a model evaluation between an ANSYS® Mechanical and a proprietary solution for rotor dynamic analysis an uncommon result drew a lot of attention: the rotor model for the commercial software shows more modes responding to an unbalance mass than the one for the Proprietary Software. This observation evidenced that for some components of the rotor it may be interesting to study the influence of considering its complete geometry instead of performing simplification through simple discs.

Those components, as like radial flow fans, or centrifugal fans (Fig. 1) have their center of mass axially displaced from their support point in the shaft that causes an asymmetry. This type of behavior is not provided in classical models for rotor dynamic analysis, as shown by Lalanne and Ferraris (2001), Genta (2005) and Bavastri et al (2008), in which rigid, symmetrical discs are inserted in the position of the center of mass of the component that is desired to be simplified.

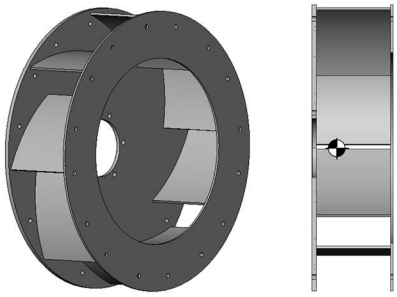

Figure 1. Classical design of a radial flow fan and its dislocated center of mass

This paper studies the effects caused by such flexible and asymmetric components with a synchronous excitation acting on the rotor and their deviations to the classic model.

2. DEVELOPMENT

2.1 Rotor dynamic models

Two different models for the calculation of rotor dynamics will be briefly presented and used for this work: the classical and the finite element models.

The classical model, developed by the Lagrangian Method in Lalanne and Ferraris (2001) and Bavastri et al (2008), which includes simplifications such as symmetric and rigid discs. In other hand, the finite element model based in commercial software ANSYS® represents a more robust and capable solution for complex models (SHARCnet, 2016), such as asymmetric and flexible discs

The first one splits a rotor into basic components such as discs, shaft and flexible bearings. Taking advantage of the Lagrange equations, Eq. (1), classical modeling is performed by defining the terms for kinetic (T) and potential energies (U) and Rayleigh's dissipation function ($\wp$) for each of the components mentioned (Bavastri et al, 2008).

$$\frac{d}{dt}\left(\frac{\partial T}{\partial \dot{q}_j}\right) - \frac{\partial T}{\partial q_j} + \frac{\partial U}{\partial q_j} + \frac{\partial \wp}{\partial \dot{q}_j} = F_{q_j} \tag{1}$$

In Eq. (1), besides the energy terms:

- F_{q_j} is the *jth* term of generalized force;
- ∂q_j and $\partial \dot{q}_j$ are the *jth* term of generalized coordinate and its time derivative, respectively.

For the disc components, assumed rigid and symmetric in all directions (Lalanne and Ferraris, 2001, and Genta, 2005), only the kinetic energy term is used. To describe its rotation, an inertial coordinate system R_0 (X, Y, Z) and a coordinate system R (x, y, z) fixed on the center of the disc, as in Fig. 2, is used. Both coordinate systems are initially coincident and are related by three angles:

- ψ, that is the rotation about Z;
- θ, that is the rotation about X;
- ϕ, that is the rotation about Y.

These are known as Euler angles and represent the angular displacements of the discs in a rotor dynamic model.

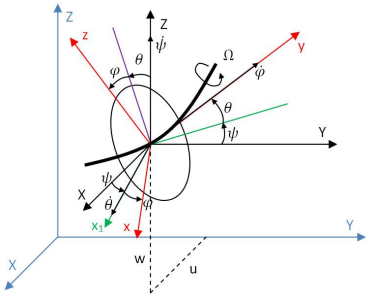

Figure 2. Euler angles relating the coordinate systems R and R_0

Assuming some linearity in the model and that the axis of rotation for the system is y and has a constant angular speed (Ω), the θ and ψ angles may be considered small (Fig. 2). Therefore, the instantaneous angular speed vector of the disc ($\overline{\omega}$), on x, y and z directions, could be defined by Eq. (2):

$$\overline{\omega} = \begin{bmatrix} \omega_x \\ \omega_y \\ \omega_z \end{bmatrix} \cong \begin{bmatrix} \dot{\psi}\,sin\phi\,cos\theta + \dot{\theta}\,cos\phi \\ -\dot{\psi}\,sin\theta + \dot{\phi} \\ \dot{\psi}\,cos\phi\,cos\theta + \dot{\theta}\,sin\phi \end{bmatrix} = \begin{bmatrix} \dot{\psi}\,sin\phi + \dot{\theta}\,cos\phi \\ -\dot{\psi}\theta + \Omega \\ \dot{\psi}\,cos\phi + \dot{\theta}\,sin\phi \end{bmatrix} \tag{2}$$

With the angular speed for the disc defined, its kinetic energy (T_D) is given by:

$$T_D = \frac{1}{2} M_D \left(\dot{u}^2 + \dot{w}^2\right) + \frac{1}{2}\left(I_{Dx}\omega_x^2 + I_{Dy}\omega_y^2 + I_{Dz}\omega_z^2\right) \tag{3}$$

where:

- M_D is the disc mass;
- $\dot{u}$ and $\dot{w}$ are the translational speed in X and Z directions, respectively;
- I_{Dx}, I_{Dy} and I_{Dz} are the transverse inertia of the disc at X, Y and Z directions, respectively;
- ω_x (or $\dot{\theta}$), ω_y (or Ω) and ω_z (or $\dot{\psi}$) are the angular speeds at X, Y and Z directions, respectively.

Then, if the disc is symmetric ($I_{Dx} = I_{Dz}$), the kinetic energy equation for discs, using Eq. (2), could be rewrite as:

$$T_D \cong \frac{1}{2} M_D \left(\dot{u}^2 + \dot{w}^2\right) + \frac{1}{2} I_{Dx} \left(\dot{\theta}^2 + \dot{\psi}^2\right) + \frac{1}{2} I_{Dy} \left(\Omega^2 + 2\Omega\dot{\psi}\theta\right) \tag{4}$$

Same procedure and assumptions are taken for the shaft, which is divided into sections, or elements, of length L. The sections are divided as need. Lalanne and Ferraris, 2001, shown that the kinetic (T_S) and the potential (U_S) energy for this shaft with length L is:

$$T_S = \frac{\rho S}{2} \int_0^L \left(\dot{u}^2 + \dot{w}^2\right) dy + \frac{\rho I}{2} \int_0^L \left(\dot{\theta}^2 + \dot{\psi}^2\right) dy + \rho L I \Omega^2 + 2\rho I \Omega \int_0^L \dot{\psi}\theta dy \tag{5}$$

$$U_S = \frac{EI}{2} \int_0^L \left[\left(\frac{\partial^2 u}{\partial y^2} \right)^2 + \left(\frac{\partial^2 w}{\partial y^2} \right)^2 \right] dy \tag{6}$$

whereas:

- ρ is the density for the shaft material;
- S is the shaft transverse area;
- I is the transverse inertia for the shaft section;
- E is the Young's Modulus for the shaft material.

The part of the bearing model will be purposely neglected in this article because of its low relevance in the subject of this. For more information on, Lalanne and Ferraris (2001), Genta (2005) or Bavastri et al (2008) shall be consulted.

Still following the classic development of Lalanne and Ferraris (2001), four degrees of freedom (DOF) are imposed at each node i of the system: two of them for displacement (u_i and w_i), and two others for rotation (θ_i and ψ_i). These four DOF set the generalized coordinate q_i that is represented by:

$$q_i = \left[u_i, w_i, \theta_i, \psi_i\right]^T \tag{7}$$

Defined the generalized coordinates, the Eq. (1) could be assembled applying the Eq. (4), (5), (6) and the bearing formulation on it. The resulting equation should be put in the frequency domain as described by Espíndola and Bavastri (1997) by using the Fourier's Transformation:

$$\left[-\Omega^2 M + i\Omega G\left(\Omega_{rpm}\right) + K\right] Q(\Omega) = F(\Omega) \tag{8}$$

where:

- M is the inertia matrix (constant and symmetrical);
- G is the gyroscopic matrix of the shaft and disc (function of rotation and skew-symmetric);
- K is the stiffness matrix for the complete dynamic rotor system (bearings, shaft and discs);
- $F(\Omega)$ is the Fourier transform of the time domain excitation;
- $Q(\Omega)$ is the Fourier transform of the time domain response;

At this point, the Eq. (8) should be solved. The analytical method for solve it involve a state space transformation for the generalized coordinates, from four to two variables, and a complex eigenvalue problem. Those will not be described on this paper but further information can be found at Espíndola and Bavastri (1997), Lalanne and Ferraris (2001) and Genta (2005).

So far, the analytical model has shown many simplifications. Genta (2005), for example, defined that the Eq. (8) applies only for "linear rotors that is axially symmetrical about its spin axis and rotates". Furthermore, the kinetic energy equation for the disc (T_D), Eq. (4), is defined assuming that the disc is symmetric. If that consideration was not done, the gyroscopic matrix G would be different considering other cross inertia terms, so like I_{XY}, and I_{XZ}. Even the mass matrix (M) changes, being now, in its sub session of inertia, composed by a full matrix and no more diagonal.

To eliminate most of these simplifying factors comes the finite element model, where is easy to considerer a complex geometry. In matter of fact, even Genta (2005) argues that a finite element model for rotor dynamic can be exceptional and achieve an unprecedented level of detail if it is robust and well done enough.

On ANSYS® documentation, the general expression of the kinetic energy for the gyroscopic matrix (E^{Gki}) for a point in element *i* with coordinates (*x*,*y*,*z*) its set as Eq. (9):

$$E^{Gki} = -\omega_x \int_{Vi} x\left(\dot{\theta}_z y + \dot{\theta}_y z\right) dm \tag{9}$$

Besides that, ANSYS® uses a complete motion equation model which considers, in addition to the mass (*M*), damping (*C*), stiffness (*K*) and gyroscopic effect (*G*) matrices, a matrix of spin softening (K_c), important for very flexible structures. This complete motion equation in matrix form is:

$$[M]\{\ddot{u}\} + ([G] + [C])\{\dot{u}\} + ([K] + [K_c])\{u\} = \{F\} \tag{10}$$

The software documentation itself lists some advantages in using the finite element model, namely:

- Accurate modeling of the mass and inertia;
- The use of the CAD geometry when meshing in solid elements;
- The ability of solid element meshes to account for the flexibility of the disc as well as the possible coupling between disc and shaft vibrations;
- The ability to include stationary parts within the full model or as substructures.

For a deeper learning and understanding about the finite element method for rotor dynamics from Genta (2005) shall be consulted.

2.2 Comparison between classical and finite element model

This paper proposes a comparison among three different methodologies: analytical model proposed by bibliography, proprietary software using the same analytical model and finite element method (FEM) using ANSYS®. These three methodologies are put side by side to solve a simple Lalanne and Ferraris (2001) example, shown in Fig. 3.

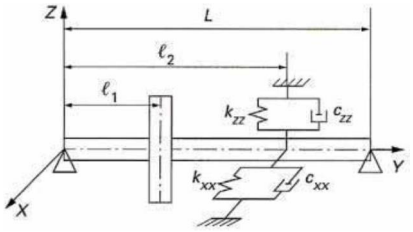

Figure 3. Geometrical model used on Lalanne and Ferraris (2001) example

The geometric parameters used in the example are presented in Tab. 1.

Table 1. Example data

Shaft data	Disc data	Spring and Dampers
Length (L) → 400 mm	Inner radius → 10 mm	Vertical Stiffness (k_{ZZ}) → 500 N/mm
Radius → 10 mm	Outer radius → 15 mm	Horizontal Stiffness (k_{XX}) → 200 N/mm
Density → 7800 kg/m³	Thickness → 30 mm	Vertical Damp (c_{ZZ}) → 0.1 Ns/mm
Young Modulus → 200 GPa	Density → 7800 kg/m³	Horizontal Danp (c_{XX}) → 0.04 Ns/mm
	Position (l_1) → $L/3$	Position (l_2) → $2L/3$

To evaluate the methodology used in the finite element model, initially, the simpler models present in the example cited will be used. Progressively, the example presented will be complicated with the inclusion of considerations such as:

- Introduction of damping and anisotropy;
- Flexible disc;
- Solid mesh for shaft and disc on the FEM model;

The first evaluation was the difference between a simple beam model with the disc consider as a mass point with its inertias and the same geometry with a shell element, both using ANSYS® and considering a rigid material for the disc (Fig. 4). From this initial test, both results were equivalent, as present in Tab. 2 and Fig. 5. Important to note that this comparison did not consider the springs and dampers, so the rotor should be named as “isotropic”.

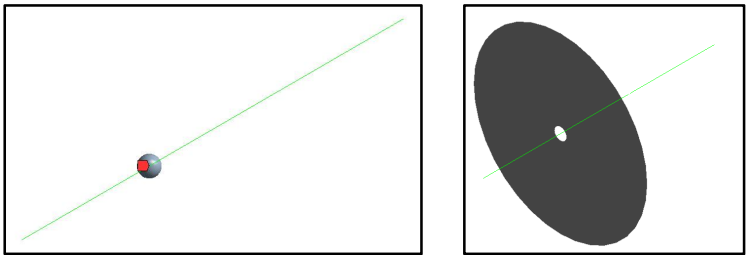

(a) (b)

Figure 4. ANSYS® simple beam model with a point of mass (a) and a surface geometry (shell element) (b) representing the disc

Table 2. Comparison of the first critical speeds for the isotropic rotor of the Lalanne and Ferraris (2001) example

	Lalanne and Ferraris (2001)	Proprietary Software	ANSYS® – Mass Point	ANSYS® – Shell Disc
1º Mode	2520 rpm	2444.48 rpm	2424.4 rpm	2422.2 rpm
2º Mode	3089 rpm	2930.59 rpm	2908.8 rpm	2906.4 rpm
3º Mode	-	5158,96 rpm	4833.6 rpm	4824.4 rpm

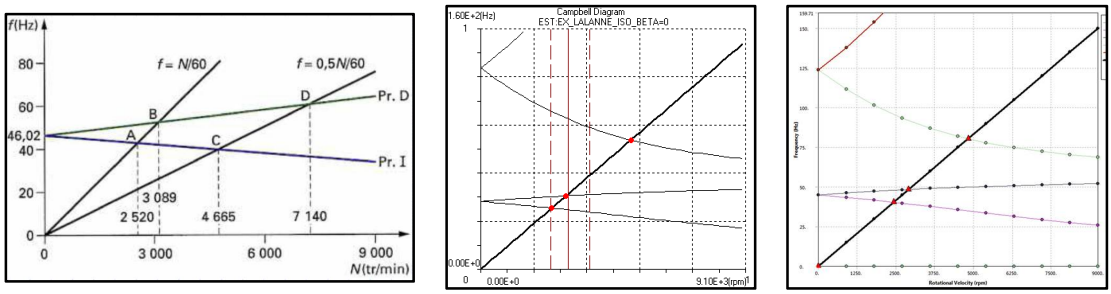

(a) (b) (c)

Figure 5. Comparison between the Campbell diagrams for the isotropic model analytical (a), Proprietary Software (b) and ANSYS® (c)

Figure 5 shows a high coherence between all the calculation methods, especially for the first two modes and between Proprietary Software and ANSYS®. Considering this result, the model to be used for validation in this work will be the one considering the shell model. Following this model, the unbalance response was compared.

For that, an unbalance mass of 0.1 g, at a radius of 150 mm, was considered in the disc The result, as showed in Fig. 6, was quite accurate showing high consistency between Proprietary Software, ANSYS® and the analytical method.

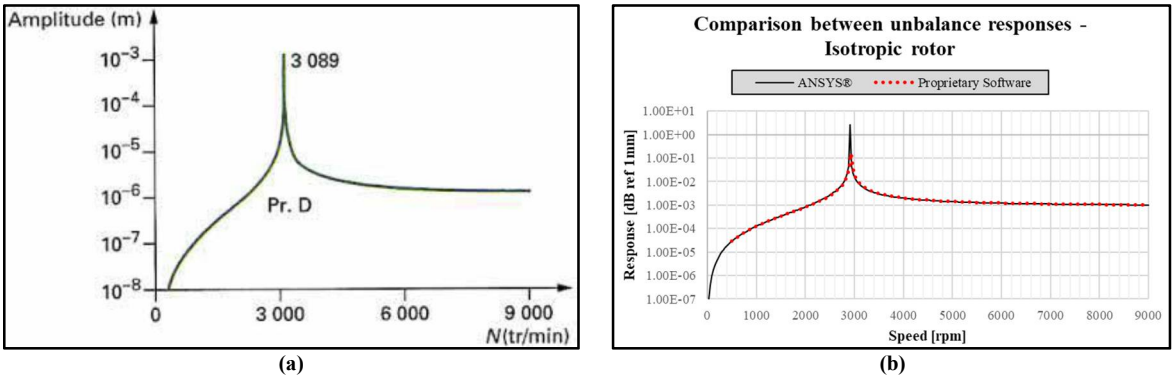

(a) (b)

Figure 6. Unbalance response calculated by analytical method (a) and the comparison between Proprietary Software and ANSYS® (b) for the isotropic rotor example

With the isotropic model validated, an anisotropic model was proposed. To do this, the springs and dampers on Tab. 1 were included for the three models. Then, the same methodology for analysis presented before was used to compare them.

Table 3. Comparison of the first critical rotations for the anisotropic rotor of the Lalanne and Ferraris (2001) example

	Lalanne and Ferraris (2001)	Proprietary Software	ANSYS®
1º Mode	2759 rpm	2650.21 rpm	2626.5 rpm
2º Mode	3431 rpm	3170.91 rpm	3145.5 rpm
3º Mode	-	5159.03 rpm	4834.2 rpm

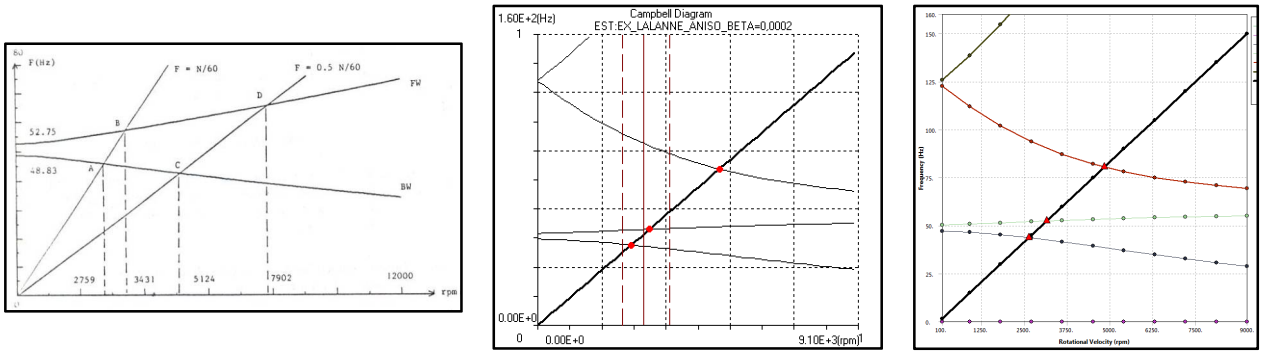

(a) (b) (c)

Figure 7. Comparison between the Campbell diagrams for the anisotropic model analytical (a), Proprietary Software (b) and ANSYS® (c)

Table 3 and Fig. 7 present that the anisotropic model shown some divergence for the second mode in the analytical model, about 300 rpm lower. On the other hand, the Proprietary Software and ANSYS® keep their high coherence. For the unbalanced response, using the same parameter used in previous case, ANSYS® starts to show its advantages, as show in Fig. 8. Neither the analytical model, nor the Proprietary Software were capable to calculate the small amplification around 4800 rpm, as detailed in Fig. 9.

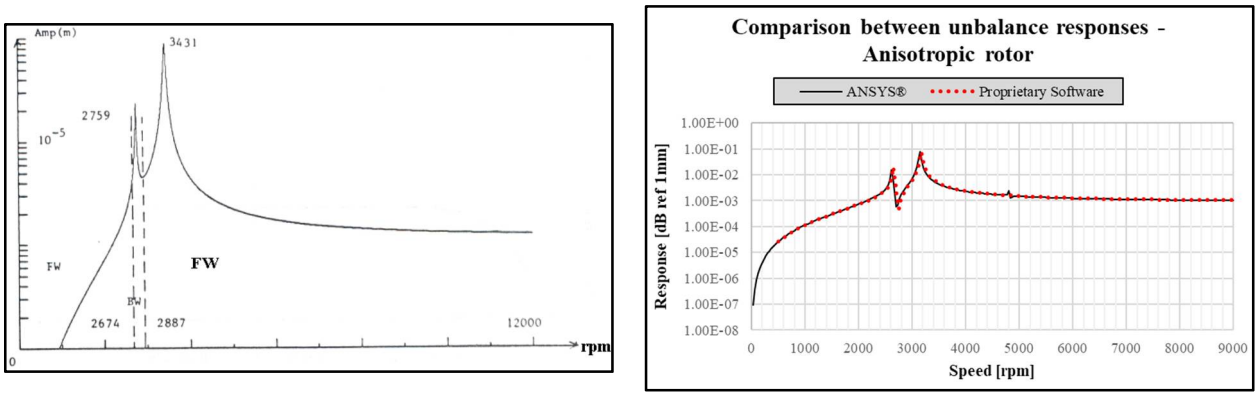

(a) (b)

Figure 8. Unbalance response calculated by analytical method (a) and the comparison between Proprietary Software and ANSYS® (b) for the anisotropic rotor example

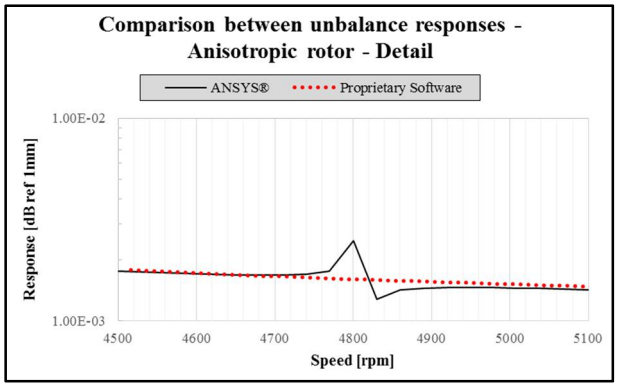

Figure 9. Detail of the amplification around 4800 rpm calculated by ANSYS®

Lastly on the validation cases, the same anisotropic model was created using solid 3D elements on ANSYS® (Fig. 10) and the result for the unbalance response was compared to the Proprietary Software, as show in Fig. 11. Two models for disc were consider in ANSYS® case: the rigid disc, and the flexible one, adding more complexity to the model, so the influence of that consideration could be evaluated.

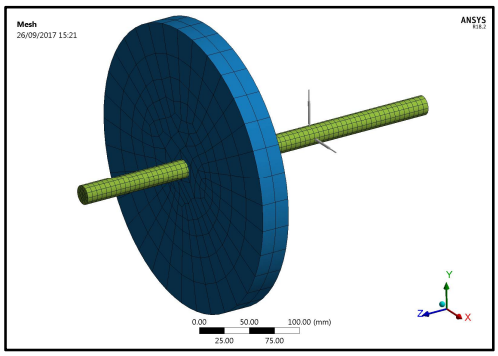

Figure 10. Solid 3D mesh for ANSYS(r) final evaluation model

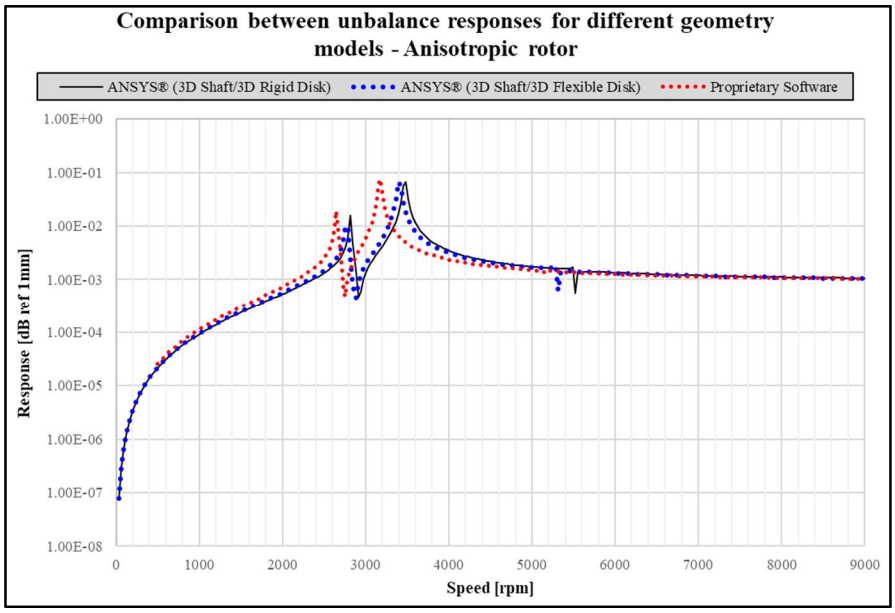

Figure 11. Difference in the unbalance response between the 3D (with rigid and flexible disc) and the classical model

As shown in Fig. 11, there is a shift between first critical rotations for the ANSYS® 3D model and the Proprietary Software analytical one. That is because the disc, when modeled as a 3D solid, causes a stiffness increase in the shaft section in which it is connected. It should be noted that the Proprietary Software presents more conservative results than

ANSYS®. Again, the commercial software results shown an additional amplification, now above 5500 rpm, caused by a disc mode at 92 Hz (Fig. 12). Both ANSYS® models, for flexible and rigid disc, show this effect.

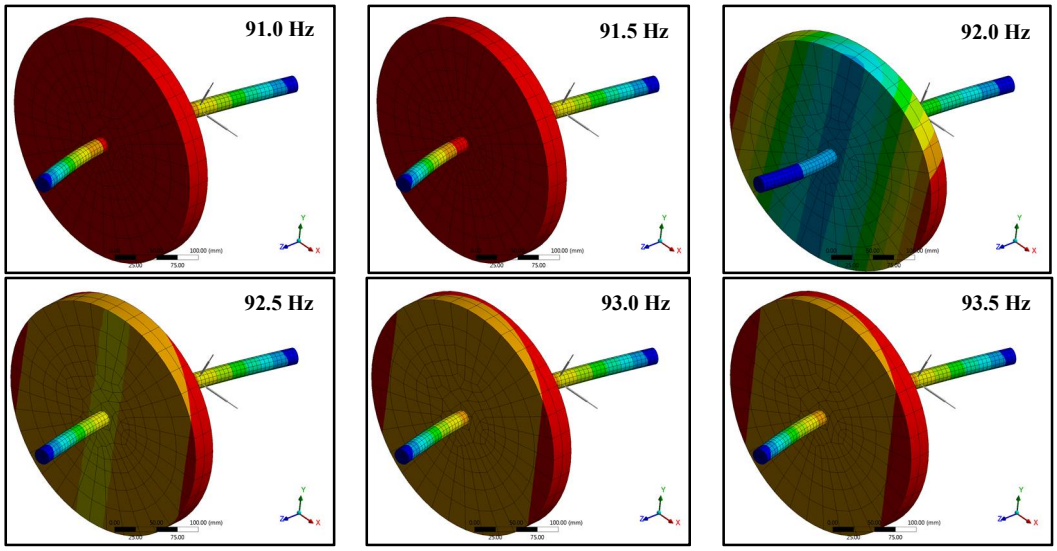

Figure 12. Progression of the angular speed going through critical speed for the disc

The results obtained so far show the ability of the Proprietary Software to perform safety calculations as well as the ability to refine such calculations via ANSYS® to visualize, and study, previously unpredictable effects.

With this in mind, and considering the appearance of modes belonging to the discs as well as their influence on the shaft response, an analysis considering the geometry of an actual rotor for a large electric motor was performed to evaluate the sensitivity of this effect in medium and large machines. In it, besides the consideration of the complete geometry of the radial fan, were considered hydrodynamic bearings, common in rotors like those that the one studied. Figure 13 shows the complete 3D model used on ANSYS®, while Fig. 14 shows the Proprietary Software model.

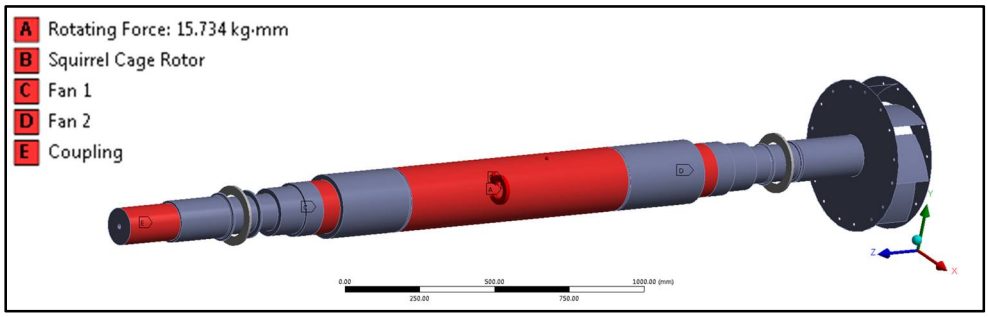

Figure 13. ANSYS® model for an electric motor rotor

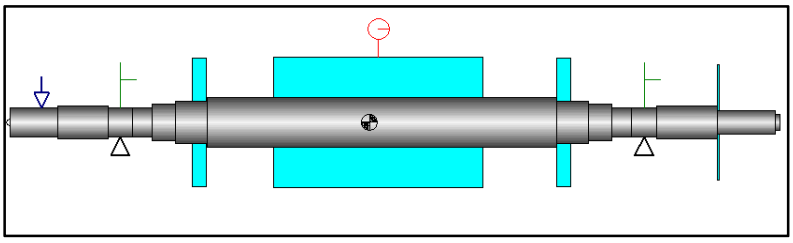

Figure 14. Proprietary Software model for an electric motor rotor

Considering an unbalance of 15734 kg.mm located at the center of the rotor package (“A” on Fig. 13 and the red symbol on Fig. 14), the response for the shaft measured at the bearing position was greatly accurately for the first two modes (horizontal and vertical) but starts to diverge after that, as show in Fig. 15. The third mode was just seem for the ANSYS® response and affect the whole system positively, reducing the vibration amplitude expected compared to that calculated by Proprietary Software, as shown in Fig. 15.

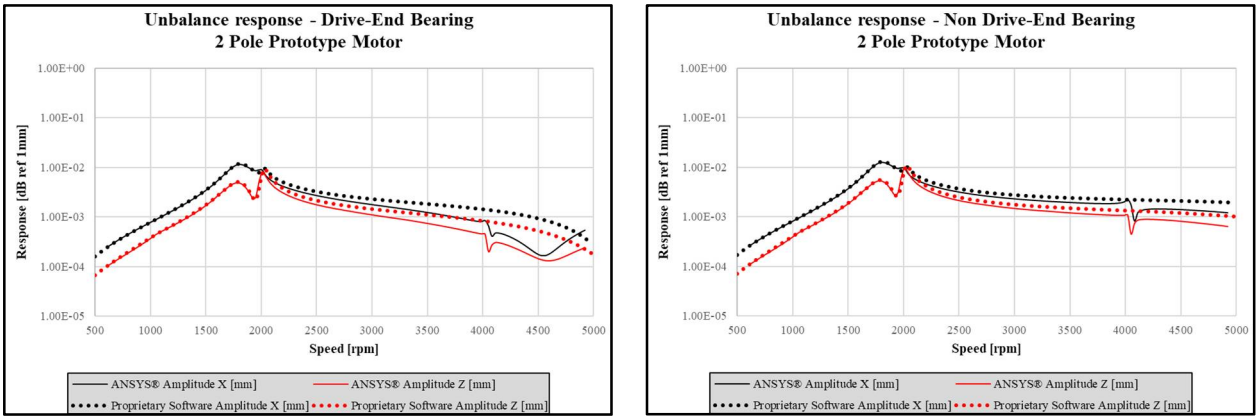

Figure 15. Comparison of the unbalance response between ANSYS® and Proprietary Software at rotor bearings

Figure 16, 17 and 18 show the vibration modes for the first three critical speeds.

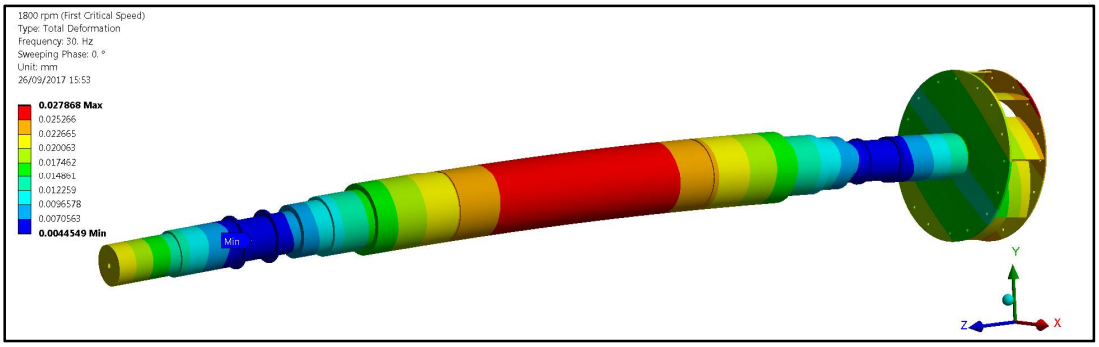

Figure 16. First critical speed (at 1800 rpm)

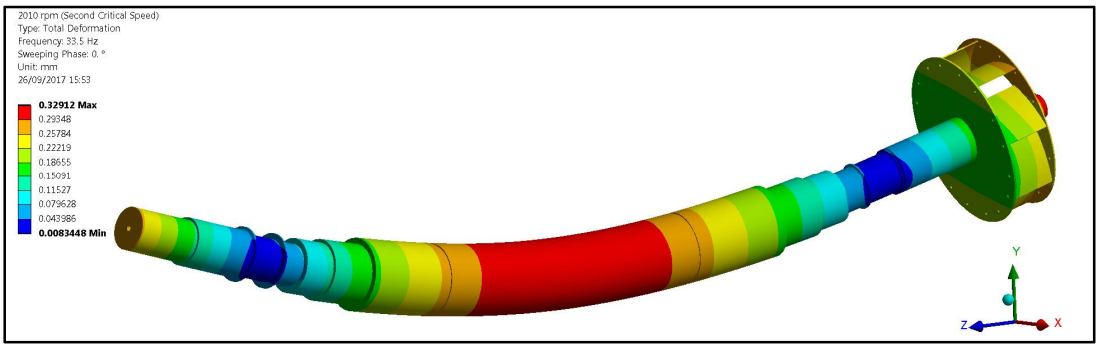

Figure 17. Second critical speed (at 2010 rpm)

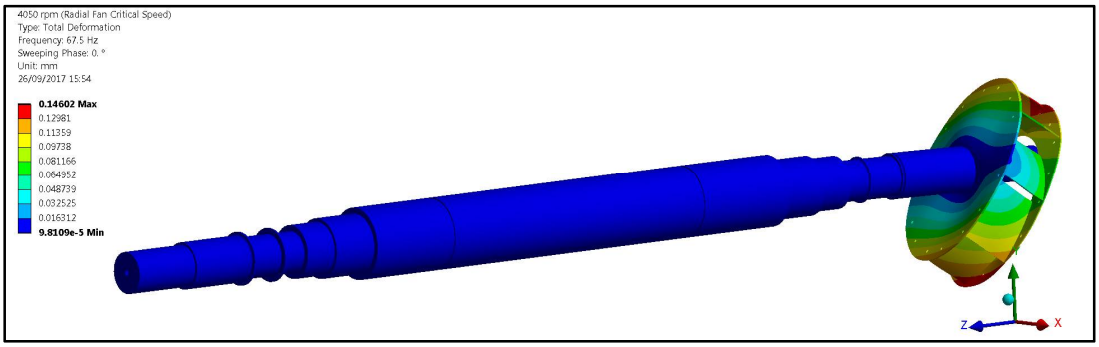

Figure 18. Radial flow fan critical speed (at 4050 rpm)

Figure 18 shows the effect of reducing the vibration levels imposed on the shaft when the radial fan is excited in its critical rotation. The analytical model does not show this effect because of its simplifications, which imply that their discs are treated as symmetrical. Besides that, the center of mass, as shown in Fig. 1, is dislocated from its support which amplify the gyroscopic effect by generating a bending force on the fan blades base plate that supports the component on the shaft.

3. CONCLUSIONS

This paper briefly presented an analytical and a finite element model for rotor dynamic analysis. These two models were compared to validate, by using a literature example, the working methodology to a rotor dynamic analysis in finite element analysis.

The comparison showed the unpredicted effect of an unbalance mass on the rotor exciting a vibration for a flexible disc coupled to it.

A model for an electric rotating machine was studied with a flexible radial flow fan coupled at its non-drive end. The results presented for this case showed the importance in considering the complete geometry on a finite element analysis when complex and flexible components are mounted on the shaft and its impact in the dynamic behavior.

4. ACKNOWLEDGEMENTS

L. G. Fonçatti and D. R. Voltolini acknowledges the support of Department of Development and Technological Innovation from WEG S.A – Energy Division.

5. REFERENCES

Bavastri, C.A., Ferreira, E.M.S., Espíndola, J.J. and Lopes, E.M.O., 2008. “Modeling of Dynamic Rotors with Flexible Bearings due to the use of Viscoelastic Materials”. In *Journal of the Brazilian Society of Mechanical Sciences and Engineering*, Vol. 30, pp 22-29.

Espíndola, J.J. and Bavastri, 1997. “An Efficient Concept of Transmissibility for a General Equipment Isolation System”. In *Proceedings of ASME Design Engineering Technical Conferences*. Sacramento, California.

Genta, G., 2005. *Dynamics of Rotating Systems. Springer*. New York, 1nd edition.

Lalanne, M. and Ferraris, G., 2001. *Rotordynamics Prediction in Engineering*. John Wiley & Sons, Inc, New York, 2nd edition.

SharcNET, 2016. “14.4 Rotating Structures”. 19 Sep. 2017 <https://www.sharcnet.ca/Software/Ansys/17.2/en-us/help/ans_thry/thy_tool19.html>.

6. RESPONSIBILITY NOTICE

The authors are the only responsible for the printed material included in this paper.